ACS OMEGA

http://pubs.acs.org/journal/acsodf

Article

Effect of Organic Solvents on a Production of PLGA-Based Drug-Loaded Nanoparticles Using a Microfluidic Device

Yi Bao, Masatoshi Maeki,* Akihiko Ishida, Hirofumi Tani, and Manabu Tokeshi*

Cite This: *ACS Omega* 2022, 7, 33079−33086

Read Online

ACCESS | Metrics & More | Article Recommendations | Supporting Information

ABSTRACT: The translation of nanoparticles (NPs) from laboratory to clinical settings is limited, which is not ideal. One of the reasons for this is that we currently have limited ability to precisely regulate various physicochemical parameters of nanoparticles. This has made it difficult to rapidly perform targeted screening of drug preparation conditions. In this study, we attempted to broaden the range of preparation conditions for particle size-modulated poly(lactic-*co*-glycolic-acid) (PLGA) NP to enhance their applicability for drug delivery systems (DDS). This was done using a variety of organic solvents and a glass-based microfluidic device. Furthermore, we compared the PDMS-based microfluidic device to the glass-based microfluidic device in terms of the possibility of a wider range of preparation conditions, especially the effect of different solvents on the size of the PLGA NPs. PLGA NPs with different sizes (sub-200 nm) were successfully prepared, and three different types of taxanes were employed for encapsulation. The drug-loaded NPs showed size-dependent cytotoxicity in cellular assays, regardless of the taxane drug used.

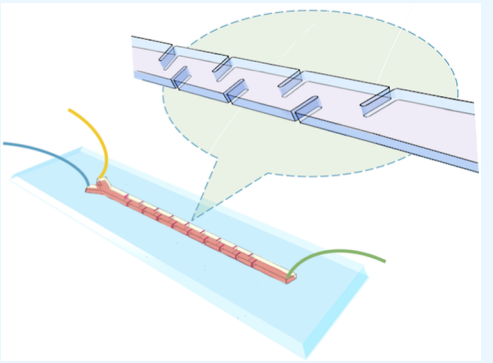

INTRODUCTION

The advent of nanoparticles (NPs) has helped to successfully overcome the inadequacies of conventional drug delivery systems (DDS); they have proven to be powerful weapons against a wide range of diseases.[1,2] NPs have been used to overcome numerous treatment obstacles.[3,4] They have demonstrated improved permeability, bioavailability, drug pharmacokinetics, stability in biological matrices, reduced adverse effects, and other features when used for drug administration.[5−9] Poly(lactic-*co*-glycolic-acid) (PLGA) polymeric NPs, in particular, are FDA-approved polymers and one of the most extensively utilized polymers in the development of nanomedicines because of their high structural integrity, tunable properties, and versatility in surface functionalization and stability.[10−12] Different functionalized innovative PLGA NPs that can target fatal cancer cells have been reported in various studies.[13−16] However, only a few formulations have been transformed into clinical applications, and only a handful have had a substantial impact. Part of the challenge lies in the complexity of optimizing the NPs because the optimal NPs parameters (surface charge, particle size, surface roughness, etc.) need to be determined according to different disease types and lesion locations.[17] In other words, to obtain finely customized DDS and tailored medications, there is still a long way to go.

The size-dependent cellular uptake in different cell lines has been widely demonstrated,[18−22] and this has greatly encouraged the advancement of size-targeted therapeutic regimens via precise particle size modulation. Microfluidic devices can precisely modulate minimal fluid volumes in microscale-controlled channels to prepare particles with controlled sizes and great batch-to-batch reproducibility.[23−30] Furthermore, microfluidic-based nanoprecipitation allows for the use of expensive therapeutics in small volumes to screen different experimental conditions and to develop optimal formulations of NP-based nanomedicines. For the preparation of NPs using the nanoprecipitation method, the solvent effect is a significant factor in controlling the NP size and encapsulating hydrophobic drugs.[31] In particular, tetrahydrofuran (THF) is widely used as a solvent to dissolve various hydrophobic materials. Therefore, in the microfluidic-based nanoprecipitation method, the use of THF as the solvent can expand NP design, including hydrophobic drug encapsulation and modification of NPs with hydrophobic materials.[32−34]

Polydimethylsiloxane (PDMS) is one of the most widely used materials in microfluidic devices.[17] However, due to the restrictive nature of PDMS, it cannot be applied to a wide range of organic reagents because of the swelling of the solvent.[35,36] Therefore, only few studies have focused on comparing the effect of solvents on the preparation of PLGA NPs in microfluidic devices. Understanding the effect of

Received: May 20, 2022
Accepted: August 22, 2022
Published: September 6, 2022

https://doi.org/10.1021/acsomega.2c03137
ACS Omega 2022, 7, 33079−33086

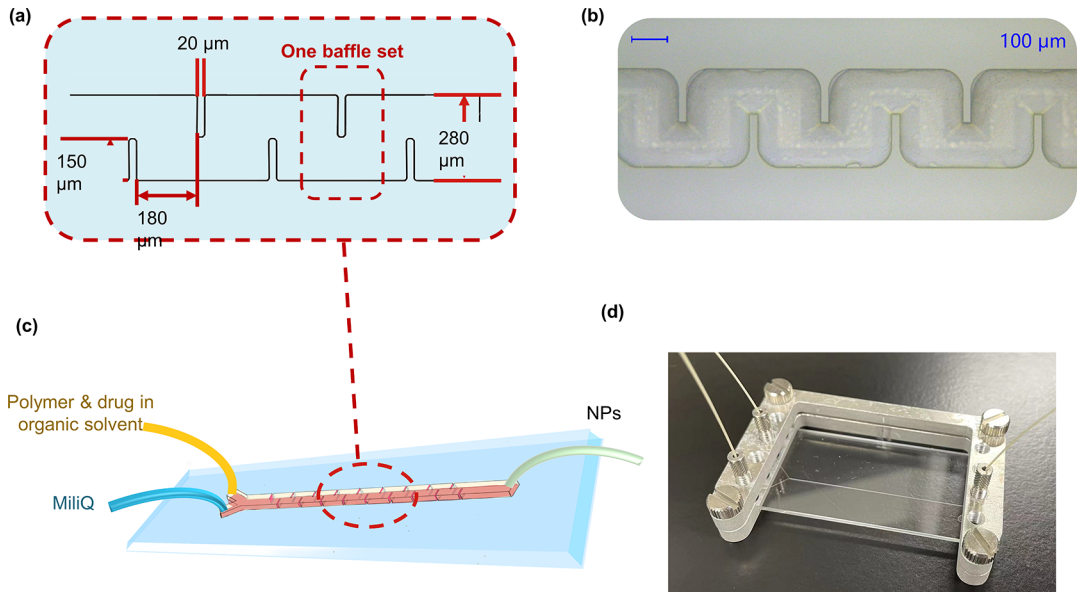

Figure 1. (a) Top view of the glass-based microfluidic device. The depth of the channel was 60 μm. The device was equipped with 20 baffle sets; (b) microscopy image of the glass device. The scale bar represents 100 μm; (c) schematics of the PLGA-based NPs preparation using the glass device. (d) Glass-based microfluidic device used in this study.

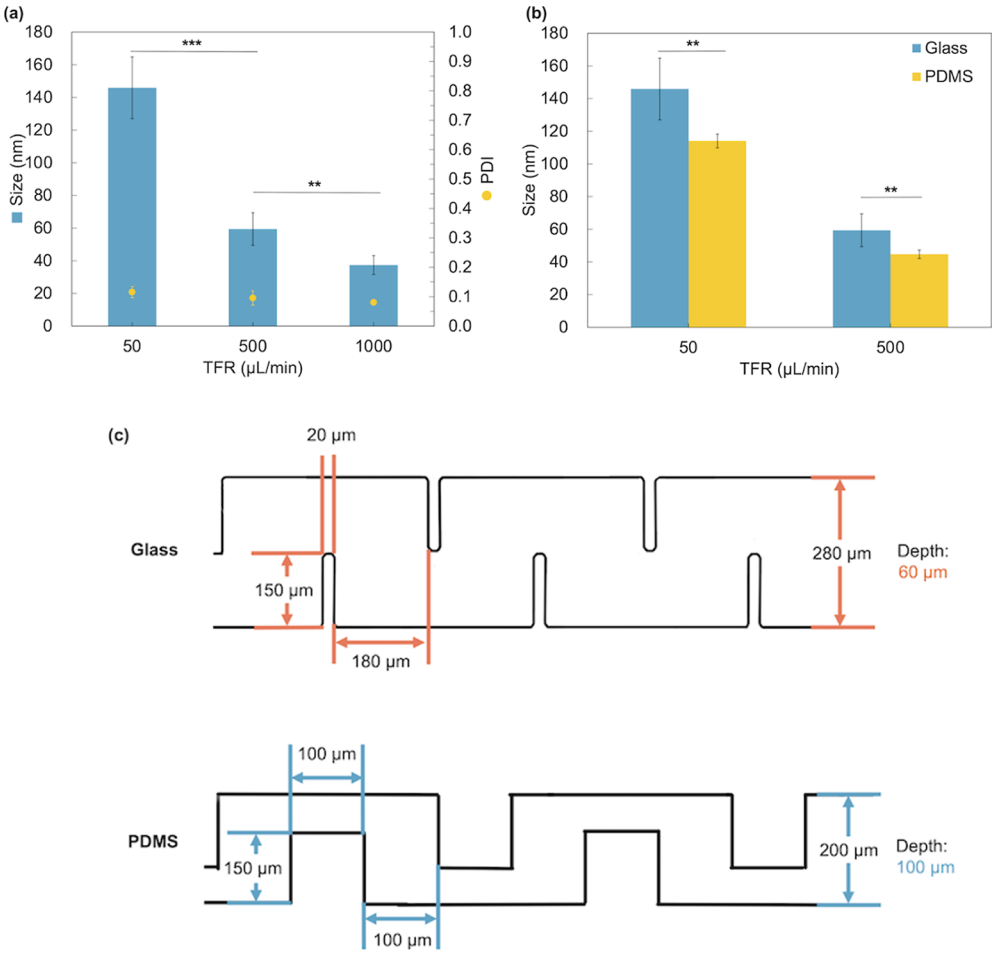

Figure 2. (a) Effect of the flow condition on PLGA NPs size in the glass device. (b) Difference between NPs prepared by the glass and PDMS microfluidic devices. (c) Comparison of the design of glass and PDMS devices. The NPs were prepared by dissolving polymers in acetonitrile at FRR 3. The standard deviations from the repeated preparation experiments were more than 3 times. *P*-values: ***≤0.0001; **≤0.001, *≤0.05. Effect of solvent properties on the PLGA NP size.

https://doi.org/10.1021/acsomega.2c03137
ACS Omega 2022, 7, 33079−33086

solvents, including THF, on PLGA NP size is essential for the development of novel PLGA-based nanomedicines.

In this study, we investigated the effects of organic solvents on the size of PLGA-NPs using a glass-based microfluidic device. Using the glass-based microfluidic device, it was possible to first evaluate the PLGA NP production behavior in the microchannel. In addition, to verify the feasibility of diverse drug encapsulation screens, we employed three distinct forms of taxanes [paclitaxel (PTX), cabazitaxel (CTX), and docetaxel (DTX)] as model drugs for encapsulation and evaluated in vitro experimental results. The prepared NPs maintained good batch-to-batch reproducibility and size-dependent cytotoxicities. The glass-based microfluidic device enables rapid optimization and screening of more favorable conditions for the preparation of NPs for DDS, accelerates clinical drug screening, and has the potential to assist rapid transfer to preclinical investigations.

RESULTS AND DISCUSSION

Effect of the Flow Condition on the PLGA NP Size. Figure 1 shows an illustration and a photograph of the microfluidic device used for PLGA NP production. The structure of the glass-based microfluidic device was based on a previous study, and it was obtained from Shin-Etsu Chemical Co., Ltd.. Here, microfluidic channels are fabricated by the typical wet etching method.[37,38] Briefly, 10% hydrofluoric acid is employed to etch the glass substrate. After the wet etching process, the glass substrate with a microchannel was aligned to a plain glass substrate with holes. The aligned glass substrates were bonded by thermal fusion bonding.

To evaluate the NP size controllability of the glass device, we produced PLGA NPs using acetonitrile as the solvent.

Figure 2a shows the PLGA NP sizes produced at the total flow rate (TFR) of 50, 500, and 1000 μL/min using a flow rate ratio (FRR; aqueous phase/organic phase) of 3. The NP size decreased from 146 nm to 37 nm when the TFR was increased from 50 to 1000 μL/min, and the NPs were able to maintain a good polydispersity index (PDI) under all flow conditions (Figure 2a). This was attributed to the more rapid solvent exchange process described in the previous work.[39] This result implies that the glass device can tolerate a higher TFR and can prepare monodisperse particles with high reproducibility in this flow rate range. As shown in Figure 2b, the NPs prepared with the glass device were larger than those obtained with the PDMS device under the same flow conditions; this was due to the difference in the microchannels caused by the device fabrication process (Figure 2c). The solvent exchange performance of the glass device was reduced compared to that of the PDMS device due to its wide microchannel structure. Overall, the results imply that the glass device can tolerate a higher TFR, produce monodisperse NPs with high reproducibility, and can be applied to produce NPs using other organic solvents.

The properties of the organic solvent affect the diffusion of the organic and aqueous phases within the microchannel, thus causing a variation in the solvent exchange time. In addition, solvent polarity is a major factor in the nanoprecipitation method used to control the NP size.[31,40,41] However, PDMS cannot use various solvents, particularly low-polarity solvents, owing to the swelling of PDMS.[35] In contrast to the PDMS device, the glass device showed high chemical resistance and could use low-polarity solvents. We conducted experiments using acetonitrile (ACN), dimethyl sulfoxide (DMSO), dimethylformamide (DMF), and THF, which are miscible with water. The important physicochemical parameters of these solvents are listed in Table 1 and are relevant for the discussion of the experimental data.

Table 1. Properties of Organic Solvents

	molecular formulas	viscosity at 25 °C (cap)	surface tension (N/m)	Hildebrand solubility parameter (MPa1/2)	polarity Index
ACN	C_2H-N	0.34	28.7	24.3	5.8
DMSO	C_2H_6OS	1.97	42.9	26.7	7.2
DMF	C_3H_7NO	0.80	36.4	24.8	6.4
THF	C_4H_8O	0.46	27.1	18.5	4.0
Water	H_2O	0.89	72	47.9	10.2

As shown in Figure 3, PLGA NP formation behavior using ACN and THF was similar, and monodisperse NPs were prepared at flow rates of 50 or 500 μL/min with good reproducibility. However, DMF and DMSO could only achieve the formation of monodispersed NPs at a low flow rate of 50 μL/min. Polydisperse NPs were formed at a TFR of 500 μL/min. The solvent parameters listed in Table 1 were related to the particle size formation. At low TFR, the NP sizes were 148 and 162 nm, respectively, when ACN and THF were used as solvents. In contrast, when DMSO and DMF were used, the NP sizes were almost 60 nm. As shown in Table 1, THF showed the lowest viscosity, surface tension, polarity, and Hildebrand solubility, and the solvent properties of ACN were similar to these. In comparison with THF and ACN, DMF and DMSO showed higher viscosity, surface tension, polarity, and Hildebrand solubility parameters. This result agrees with previous reports where PLGA NPs were prepared by nanoprecipitation.[31,39,42]

In addition, at a high TFR, the low repeatability or wide size distribution was attributed to the high viscosity and high surface tension of DMSO and DMF. As explained by the principle of the two-block polymer NPs' mechanism in microfluidic devices, the solvent exchange time (mixing time) of the organic solvent with water is essential,[39] and the high viscosity, surface tension, and polarity of the organic solvent would cause a slower solvent change in the microchannel during the NP formation process, which results in the formation of large-sized NPs or aggregates. From the fluid dynamics in the microchannel and solvent properties, we considered the difference in the PLGA formation behavior between the TFR of 50 and 500 μL/min conditions when DMSO and DMF were the solvents. The polarity of solvents was rapidly increased by mixing with the water, particularly the TFR of the 500 μL/min condition. Therefore, some PLGA molecules were immediately self-assembled to form NPs and formed small-sized NPs. However, other organic solvent properties such as viscosity and surface tension affected the mixing efficiency of the microfluidic device and formed the large-sized NPs. In contrast, the mixing efficiency of the microfluidic device at 50 μL/min was not enough to form small-sized NPs, and monodispersed large-sized NPs were produced by the slow solvent dilution. Based on these results, the screening range for size-modulated NPs preparation conditions may be enlarged, especially for a broader range of solvents. This will be resulting in a rapid and broad range of DDS screening and a significant step forward in later clinical settings.

https://doi.org/10.1021/acsomega.2c03137
ACS Omega 2022, 7, 33079−33086

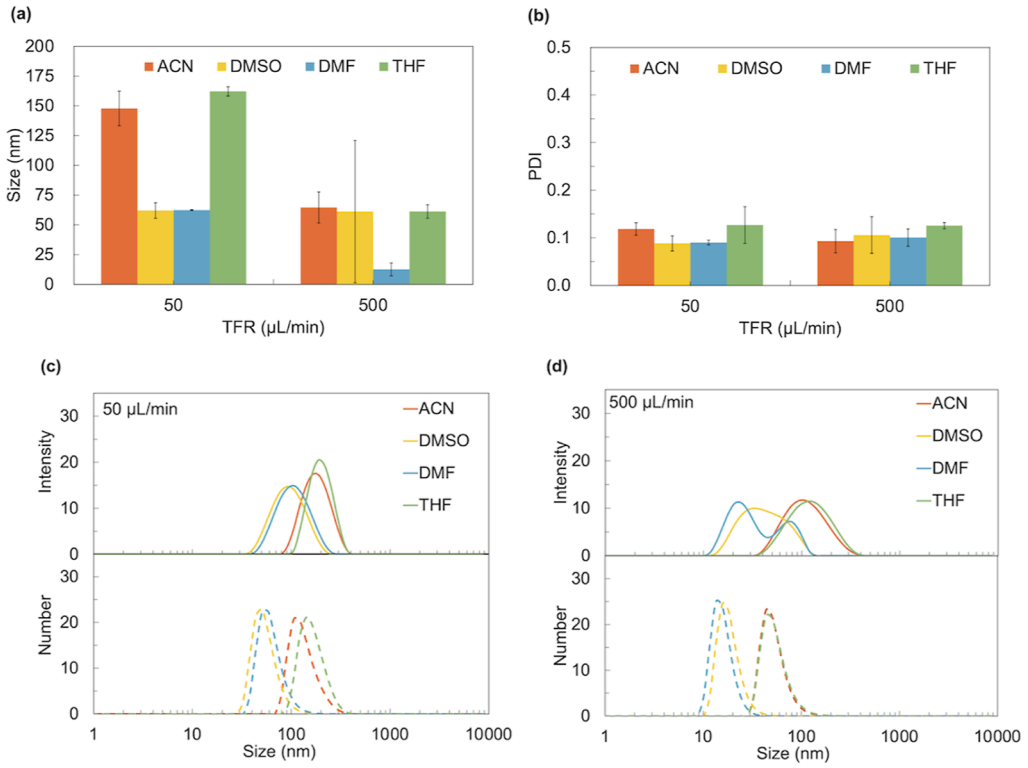

Figure 3. (a) Effect of the solvent properties on number-weighted NP size when the TFF is 50 or 500 μL/min; (b) PDI of prepared NPs; (c,d) NP size distribution prepared by four kinds of solvents: ACN, DMSO, DMF, and THF. Solid lines represent the size distribution of intensity, while the dotted lines are numbers. The error bar represents the standard deviations from repeated experiments (at least three times). ACN (acetonitrile), DMSO (dimethyl sulfoxide), DMF (dimethylformamide), and THF (tetrahydrofuran).

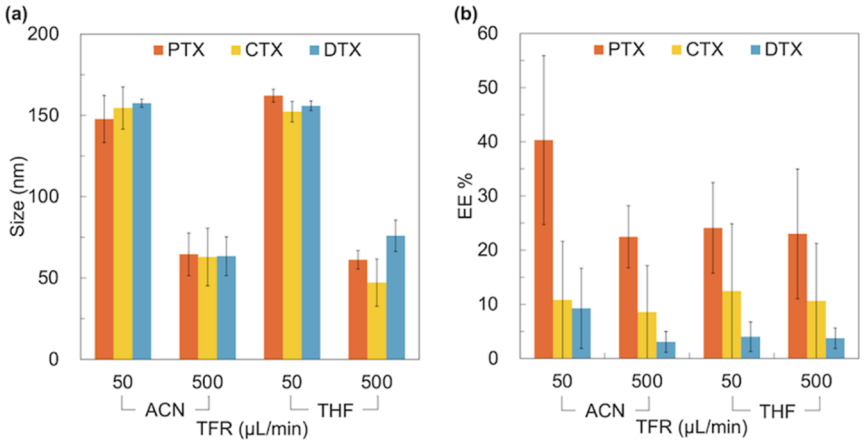

Figure 4. Difference of TFR or solvent on different kinds of drug-encapsulated NPs. (a) NPs size of PLGA-based NPs encapsulate PTX/CTX/DTX by employing ACN or THF as the solvent; (b) EE of drug-loaded NPs. The standard deviations were calculated from repeated preparation experiments that were more than three times higher. ACN (acetonitrile) and THF (tetrahydrofuran). Effect of PLGA NP size on cytotoxicity.2

Encapsulation of Different Kinds of Anti-cancer Drugs. Three different taxanes (PTX, CTX, and DTX) were used as model drugs. PTX and DTX are semisynthetic derivatives of 10-deacetylbaccatin-III. The natural PTX precursor molecule can be extracted from the European yew tree easily and sustainably. CTX, a novel second-generation taxane, is a dimethyl derivative of DTX bearing methoxy groups in place of the hydroxyl groups at the C-7 and C-10 positions.

ACN or THF was used as the solvent to prepare NPs with a concentration of 5 mg/mL of polymer, and the concentration of the drug being encapsulated was 0.5 mg/mL (10% of polymer). Similar to PTX-encapsulated NPs, CTX- and DTX-encapsulated NPs also decreased in size with increasing TFR, and no effect of solvent type on NP size was observed (Figure 4a). The encapsulation efficacies (EEs) of the three different drugs in the NPs are shown in Figure 4b. The EE of PTX was higher than that of CTX and DTX, regardless of TFR conditions. This can be attributed to PTX having the highest molecular weight. For the same mass concentration, a higher molecular weight means a lower amount of substance, and thus, less unencapsulation in the polymeric NPs; this implies a higher EE. In addition, the higher hydrophobicity of PTX

https://doi.org/10.1021/acsomega.2c03137
ACS Omega 2022, 7, 33079−33086

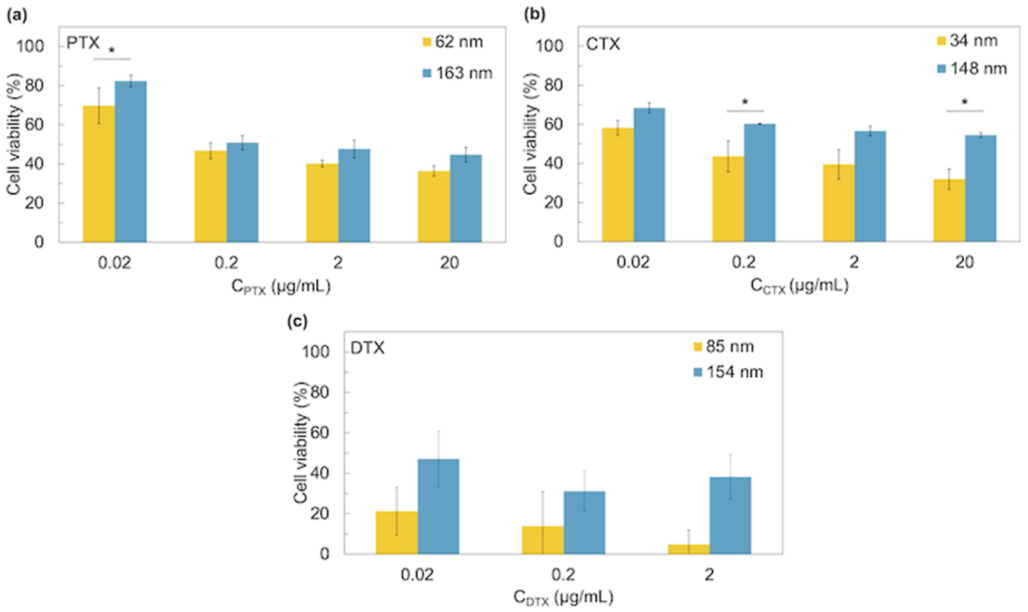

Figure 5. NP size effect on HeLa cell viability by incubated 24 h. (a) PTX-loaded NPs; (b) CTX-loaded NPs; (c) DTX-loaded NPs. Standard deviations were calculated from the repeated experiment more than three times. *P*-values: *≤0.05.

compared with other drugs is one of the reasons for its higher EE.

Particles with different NP sizes were prepared to confirm that size-modulated NPs are useful for screening future DDS for clinical use. We used THF as the solvent; however, THF is not appropriate for the PDMS device. The NP size was modulated by varying only the TFR (50 or 500 μL/min) and encapsulating different types of taxane (PTX, CTX, and DTX) anticancer drugs. These three drugs have similar mechanisms of action: binding to microtubule proteins and impairing the natural dynamics of microtubules, leading to mitotic arrest and apoptosis.[43−45]

As shown in Figure 5, NPs encapsulated with the three different types of anticancer drugs showed NP size-dependent cell growth inhibition in HeLa cells after 24 h of incubation at drug concentrations ranging from 0.02 to 20 μg/mL. In HeLa cells incubated with PTX-loaded NPs, the cell viability of those incubated with 62 nm NPs decreased from approximately 70% to approximately 36% with increasing PTX concentration, while that of cells incubated with 163 nm NPs decreased from 82 to 45%. The results for CTX-loaded NPs were similar to those for PTX; with increasing CTX concentrations, the cell viability decreased from 58 to 32% with 34 nm NPs and from 68 to 55% with 148 nm NPs. For DTX-NPs, the viability of HeLa cells incubated with 85 nm NPs decreased from 21 to 5%, while that with 154 nm NPs decreased from 47 to 38%. Overall, smaller NPs showed greater cytotoxicity. It has been previously shown that PLGA has a particle size effect on cellular uptake.[19,46,47] However, few studies focusing on in vitro NP size effects using the NPs prepared by the same polymer precursors. Our study fills this knowledge gap. Furthermore, our study demonstrated the ability of the glass-based microfluidic device to broaden the range of NPs preparation conditions, especially solvent conditions, compared to those using PDMS devices. These results strongly demonstrate the great potential of the glass-based microfluidic device as a large-scale screening device for the preparation of NPs for DDS and the establishment of a particle-size-controllable DDS.

CONCLUSIONS

In this study, we have explored the effect of condition, mainly for different organic solvents, for preparing size-modulated sub-200 nm PLGA NPs using a glass microfluidic device, without changing the polymer precursors. We also demonstrated the NP production of taxane-based anticancer drugs as model polymers and model pharmaceuticals. More specifically, under the preparative conditions of this study, ACN and THF were more suitable for preparing size-modulated NPs with narrower particle size distributions. In addition, PTX had a higher EE than CTX and DTX. Our results also showed the particle size impact of NPs on HeLa cells, regardless of the type of drug used in the in vitro studies. We believe that the glass-based microfluidic device will serve as a powerful tool for effectively advancing drug screening and enbling tailored therapeutics in the future.

EXPERIMENTAL SECTION

Materials. PLGA (50:50 ratio, Mw = 24000−38000 Da) and PEG-PLGA (average Mn_{PEG} = 2000 Da, average Mn_{PLGA} = 11500 Da) were obtained from Sigma-Aldrich (St. Louis, MO, USA). PTX, COX, and DOX were purchased from Tokyo Chemical Industry Ltd. (Tokyo, Japan). Acetonitrile (ACN), dimethyl sulfoxide (DMSO), dimethylformamide (DMF), and tetrahydrofuran (THF) were purchased from FUJIFILM Wako Pure Chemical Corporation (Osaka, Japan).

Preparation of Polymeric NPs. A 5 mg/mL mixture of PLGA and PEG-PLGA with a mass ratio of 1:1; and 0.5 mg/mL of different kinds of anti-cancer drugs (10% of polymer) were dissolved in an organic solvent. The syringes were connected to the microfluidic device, and the organic solution was fed with ultrapure water into the microfluidic device from two different inlets using syringe pumps (LEGATO 210; KD Scientific Inc., Hollistion, MA, USA). The collected solution was dialyzed overnight in ultrapure water through a membrane bag (MWCO:12−14 kD; Spectrum Laboratories, Inc., Canada) to remove the organic solvent. The sizes of the

https://doi.org/10.1021/acsomega.2c03137
ACS Omega 2022, 7, 33079−33086

NPs were evaluated using dynamic light scattering (DLS. Zetasizer nano ZS ZEN360; Malvern Instruments, UK).

Determination of the Encapsulation Efficiency. The drug content of the NPs was determined using HPLC (HITACHI, Japan). The NP solution was freeze-dried to a powder, which was then dissolved in ACN. For PTX and DTX, the mobile phase consisted of ACN and water (50:50 v/v) and a reverse-phase column was used to maintain a temperature of 30 °C. The flow rate was 1.2 mL/min, and the UV detection wavelength was 227 nm. CTX was ACN: water = 58:42 (v/v), the flow rate was 1.0 mL/min, and the UV detection wavelength was 228 nm.

The HPLC was calibrated using a standard solution containing 5−100 μg/mL of the drug in CAN (Figure S1). The encapsulation efficiency (EE) can be determined by the ratio of the amount of drug inside the sample solution to the amount of drug used for NPs preparation (eq 1)

$$\text{EE}\ (\%) = \frac{\text{Amount of drugs in NPs}}{\text{The total amount of drug}} \times 100\% \quad (1)$$

Cell Viability. Human cervical cancer HeLa cells were grown in Dulbecco's modified essential medium (DMEM, Sigma-Aldrich, St. Louis, MO, USA) supplemented with 10% (v/v) fetal bovine serum (FBS) and 1% penicillin−streptomycin. The cells were maintained in a humidified atmosphere containing 5% CO_2 at 37 °C in an incubator.

The cells were seeded in 96-well plates at a density of 5000 cells/well. After the cells adhered to the wall of the plate, NPs were added and incubated with at least three replicate wells per group for a certain period. After incubation, cytotoxicity was assayed by adding 10 μL of Cell Counting kit-8 (CCK-8, Dojindo, Japan) solution. The plates were further incubated for 1 h before measuring absorbance at 450 nm using a microplate reader (Infinite-M Nano 200 Pro, TECAN, Switzerland). Equation 2 was employed to determine cell viability.

$$\text{Cell viability}\ (\%) = \frac{A_{\text{sample}} - A_{\text{negative}}}{A_{\text{positive}} - A_{\text{negative}}} \times 100\% \quad (2)$$

where A_{sample}, A_{positive}, and A_{negetive} are the absorbance of the sample, positive control, and negative control, respectively.

Statistical Analysis. The results are expressed as the mean ± standard deviation and were analyzed using T-TEST to demonstrate statistical differences. A predictive value (P) ≤ 0.05 was statistically significant.

■ ASSOCIATED CONTENT

Supporting Information

The Supporting Information is available free of charge at https://pubs.acs.org/doi/10.1021/acsomega.2c03137.

Standard Curve and Correlation Equation of drug determined by HPLC (PDF)

■ AUTHOR INFORMATION

Corresponding Authors

Masatoshi Maeki − *Division of Applied Chemistry, Faculty of Engineering, Hokkaido University, Sapporo 060-8628, Japan; JST PRESTO, Kawaguchi, Saitama 332-0012, Japan;* orcid.org/0000-0001-7500-4231; Phone: +81-706-6773; Email: m.maeki@eng.hokudai.ac.jp; Fax: +81-11-706-6745

Manabu Tokeshi − *Division of Applied Chemistry, Faculty of Engineering, Hokkaido University, Sapporo 060-8628, Japan;* orcid.org/0000-0002-4412-2144; Phone: +81-11-706-6744; Email: tokeshi@eng.hokudai.ac.jp; Fax: +81-11-706-6745

Authors

Yi Bao − *Graduate School of Chemical Sciences and Engineering, Hokkaido University, Sapporo 060-8628, Japan*

Akihiko Ishida − *Division of Applied Chemistry, Faculty of Engineering, Hokkaido University, Sapporo 060-8628, Japan;* orcid.org/0000-0003-4100-9426

Hirofumi Tani − *Division of Applied Chemistry, Faculty of Engineering, Hokkaido University, Sapporo 060-8628, Japan;* orcid.org/0000-0002-5935-0756

Complete contact information is available at: https://pubs.acs.org/10.1021/acsomega.2c03137

Author Contributions

Conceptualization: M.M. and M.T.; data curation: Y.B.; formal analysis: Y.B.M. M, A.I., and H.T.; methodology: Y.B. and M.M.; investigation: Y.B. and M.M.; writing-original draft: Y·B.; writing-review and editing: M.M. and M.T.; funding acquisition: M.M. and M.T.; resources: Y.B. and M.M.; supervision: M.M. and M.T. The manuscript was written through the contributions of all authors. All the authors approved the final version of the manuscript.

Notes

The authors declare no competing financial interest.

■ ACKNOWLEDGMENTS

This work was supported by JST, CREST (Grant Number JPMJCR17H1), JST, PRESTO (Grant Number JPMJPR19K8), Special Education and Research Expenses from the Ministry of Education, Culture, Sports, Science, and Technology, AMED (grant number JP21zf0127004), JSPS KAKENHI (Grant Number JP19KK0140), Hokkaido University Support Program for Frontier Research, Hosokawa Powder Technology Foundation, and Iketani Science and Technology Foundation.

■ ABBREVIATIONS

abrNPs, nanoparticle; DDS, drug delivery system; PLGA, poly(lactic-*co*-glycolic-acid); PEG, polyethylene glycol; ACN, acetonitrile; DMSO, dimethyl sulfoxide; DMF, dimethylformamide; THF, tetrahydrofuran; EE, encapsulation efficiency; PTX, paclitaxel; CTX, cabazitaxel; DTX, docetaxel; TFR, total flow rate; FRR, flow ratio rate; LNPs, lipid nanoparticles; HPLC, high-performance liquid chromatography; MW, molecular weight; DLS, dynamic light scattering; DMEM, Dulbecco's modified Eagle's medium; FBS, fetal bovine serum; PDMS, polydimethylsiloxane

■ REFERENCES

(1) Sanjay, S. T.; Zhou, W.; Dou, M.; Tavakoli, H.; Ma, L.; Xu, F.; Li, X. J. Recent Advances of Controlled Drug Delivery Using Microfluidic Platforms. *Adv. Drug Delivery Rev.* **2018**, *128*, 3−28.

(2) Sanjay, S. T.; Maowei, D.; Guanglei, F.; Feng, X.; Xiujun, L. Controlled Drug Delivery Using Microdevices: Ingenta Connect. *Curr. Pharmaceut. Biotechnol.* **2016**, *17*, 772−787.

(3) Thomas, O. S.; Weber, W. Overcoming Physiological Barriers to Nanoparticle Delivery—Are We There Yet? *Front. Bioeng. Biotechnol.* **2019**, *7*, 415.

(4) Moura, R. P.; Martins, C.; Pinto, S.; Sousa, F.; Sarmento, B. Blood-Brain Barrier Receptors and Transporters: An Insight on Their Function and How to Exploit Them through Nanotechnology. *Expet Opin. Drug Deliv.* **2019**, *16*, 271−285.
(5) Sur, S.; Rathore, A.; Dave, V.; Reddy, K. R.; Chouhan, R. S.; Sadhu, V. Recent Developments in Functionalized Polymer Nanoparticles for Efficient Drug Delivery System. *Nano-Struct. Nano-Objects* **2019**, *20*, 100397.
(6) Wilczewska, A. Z.; Niemirowicz, K.; Markiewicz, K. H.; Car, H. Nanoparticles as Drug Delivery Systems. *Pharmacol. Rep.* **2012**, *64*, 1020−1037.
(7) Riehemann, K.; Schneider, S. W.; Luger, T. A.; Godin, B.; Ferrari, M.; Fuchs, H. Nanomedicine-Challenge and Perspectives. *Angew. Chem., Int. Ed.* **2009**, *48*, 872−897.
(8) Lepeltier, E.; Bourgaux, C.; Couvreur, P. Nanoprecipitation and the "Ouzo effect": Application to drug delivery devices *Advanced Drug Delivery Reviews*; Elsevier May 1, 2014, Vol *71*, pp 86−97.
(9) McNeil, S. E. Nanotechnology for the Biologist. *J. Leukocyte Biol.* **2005**, *78*, 585−594.
(10) Danhier, F.; Ansorena, E.; Silva, J. M.; Coco, R.; Le Breton, A.; Préat, V. PLGA-Based Nanoparticles: An Overview of Biomedical Applications. *J. Controlled Release* **2012**, *161*, 505−522.
(11) Kumari, A.; Yadav, S. K.; Yadav, S. C. Biodegradable Polymeric Nanoparticles Based Drug Delivery Systems. *Colloids Surf., B* **2010**, *75*, 1−18.
(12) Pandita, D.; Kumar, S.; Lather, V. Hybrid Poly(Lactic-Co-Glycolic Acid) Nanoparticles: Design and Delivery Prospectives. *Drug Discovery Today* **2015**, *20*, 95−104.
(13) Zhang, Z.; Wang, X.; Li, B.; Hou, Y.; Yang, J.; Yi, L. Development of a Novel Morphological Paclitaxel-Loaded PLGA Microspheres for Effective Cancer Therapy: In Vitro and in Vivo Evaluations. *Drug Delivery* **2018**, *25*, 166−177.
(14) Acharya, S.; Sahoo, S. K. PLGA Nanoparticles Containing Various Anticancer Agents and Tumour Delivery by EPR Effect. *Adv. Drug Delivery Rev.* **2011**, *63*, 170−183.
(15) Cheng, J.; Teply, B. A.; Sherifi, I.; Sung, J.; Luther, G.; Gu, F. X.; Levynissenbaum, E.; Radovicmoreno, A. F.; Langer, R.; Farokhzad, O. C. Formulation of Functionalized PLGA-PEG Nanoparticles for in Vivo Targeted Drug Delivery. *Biomaterials* **2007**, *28*, 869−876.
(16) Bhardwaj, V.; Ankola, D. D.; Gupta, S. C.; Schneider, M.; Lehr, C. M.; Kumar, M. N. V. R. PLGA Nanoparticles Stabilized with Cationic Surfactant: Safety Studies and Application in Oral Delivery of Paclitaxel to Treat Chemical-Induced Breast Cancer in Rat. *Pharm. Res.* **2009**, *26*, 2495−2503.
(17) Zhou, W.; Dou, M.; Timilsina, S. S.; Xu, F.; Li, X. J. Recent Innovations in Cost-Effective Polymer and Paper Hybrid Microfluidic Devices. *Lab Chip* **2021**, *21*, 2658−2683.
(18) Chiu, H. I.; Samad, N. A.; Fang, L.; Lim, V.; Royal Society of Chemistry February, 2021; Vol. *11*, pp 9433−9449.Cytotoxicity of Targeted PLGA Nanoparticles: A Systematic Review*RSC Adv.* DOI: 10.1039/d1ra00074h
(19) Choi, J. S.; Cao, J.; Naeem, M.; Noh, J.; Hasan, N.; Choi, H. K.; Yoo, J. W. Size-Controlled Biodegradable Nanoparticles: Preparation and Size-Dependent Cellular Uptake and Tumor Cell Growth Inhibition. *Colloids Surf., B* **2014**, *122*, 545−551.
(20) Breunig, M.; Bauer, S.; Goepferich, A.; Elsevier January, 2008; Vol. *68*, pp 112−128.Polymers and Nanoparticles: Intelligent Tools for Intracellular Targeting?*Eur. J. Pharm. Biopharm.* DOI: 10.1016/j.ejpb.2007.06.010
(21) Madani, F.; Esnaashari, S. S.; Mujokoro, B.; Dorkoosh, F.; Khosravani, M.; Adabi, M. Investigation of Effective Parameters on Size of Paclitaxel Loaded PLGA Nanoparticles. *Adv. Pharm. Bull.* **2018**, *8*, 77−84.
(22) Shah, N.; Chaudhari, K.; Dantuluri, P.; Murthy, R. S. R.; Das, S. Paclitaxel-Loaded PLGA Nanoparticles Surface Modified with Transferrin and Pluronic®P85, an in Vitro Cell Line and in Vivo Biodistribution Studies on Rat Model. *J. Drug Targeting* **2009**, *17*, 533−542.
(23) Rhee, M.; Valencia, P. M.; Rodriguez, M. I.; Langer, R.; Farokhzad, O. C.; Karnik, R. Synthesis of Size-Tunable Polymeric Nanoparticles Enabled by 3D Hydrodynamic Flow Focusing in Single-Layer Microchannels. *Adv. Mater.* **2011**, *23*, H79−H83.
(24) Valencia, P. M.; Basto, P. A.; Zhang, L.; Rhee, M.; Langer, R.; Farokhzad, O. C.; Karnik, R. Single-Step Assembly of Homogenous Lipid−Polymeric and Lipid−Quantum Dot Nanoparticles Enabled by Microfluidic Rapid Mixing. *ACS Nano* **2010**, *4*, 1671−1679.
(25) Damiati, S.; Kompella, U. B.; Damiati, S. A.; Kodzius, R. *MDPI AG February* **2018**, *9*, 103.
(26) Maeki, M.; Okada, Y.; Uno, S.; Niwa, A.; Ishida, A.; Tani, H.; Tokeshi, M. Production of SiRNA-Loaded Lipid Nanoparticles Using a Microfluidic Device. *J. Visualized Exp.* **2022**, *181*, 5671.
(27) Maeki, M.; Uno, S.; Niwa, A.; Okada, Y.; Tokeshi, M. Microfluidic Technologies and Devices for Lipid Nanoparticle-Based RNA Delivery. *J. Controlled Release* **2022**, *344*, 80−96.
(28) Kimura, N.; Maeki, M.; Sasaki, K.; Sato, Y.; Ishida, A.; Tani, H.; Harashima, H.; Tokeshi, M. Three-Dimensional, Symmetrically Assembled Microfluidic Device for Lipid Nanoparticle Production. *RSC Adv.* **2021**, *11*, 1430−1439.
(29) Dou, M.; García, J. M.; Zhan, S.; Li, X. J. Interfacial Nano-Biosensing in Microfluidic Droplets for High-Sensitivity Detection of Low-Solubility Molecules. *Chem. Commun.* **2016**, *52*, 3470−3473.
(30) Lv, M.; Zhou, W.; Tavakoli, H.; Bautista, C.; Xia, J.; Wang, Z.; Li, X. J. Aptamer-Functionalized Metal-Organic Frameworks (MOFs) for Biosensing. *Biosens. Bioelectron.* **2021**, *176*, 112947.
(31) López, R. R.; Font de Rubinat, G. P.; Sánchez, L. M.; Tsering, T.; Alazzam, A.; Bergeron, K. F.; Mounier, C.; Burnier, J. V.; Stiharu, I.; Nerguizian, V. The Effect of Different Organic Solvents in Liposome Properties Produced in a Periodic Disturbance Mixer: Transcutol®, a Potential Organic Solvent Replacement. *Colloids Surf., B* **2021**, *198*, 111447.
(32) Wischke, C.; Schwendeman, S. P. Principles of Encapsulating Hydrophobic Drugs in PLA/PLGA Microparticles. *Int. J. Pharm.* **2008**, *364*, 298−327.
(33) Lepeltier, E.; Bourgaux, C.; Couvreur, P. Nanoprecipitation and the "Ouzo Effect": Application to Drug Delivery Devices. *Adv. Drug Delivery Rev.* **2014**, *71*, 86−97.
(34) Allen, C.; Maysinger, D.; Eisenberg, A. Nano-Engineering Block Copolymer Aggregates for Drug Delivery. *Colloids Surf., B* **1999**, *16*, 3−27.
(35) Lee, J. N.; Park, C.; Whitesides, G. M. Solvent Compatibility of Poly(Dimethylsiloxane)-Based Microfluidic Devices. *Anal. Chem.* **2003**, *75*, 6544−6554.
(36) Toepke, M. W.; Beebe, D. J. PDMS Absorption of Small Molecules and Consequences in Microfluidic Applications. *Lab Chip* **2006**, *6*, 1484−1486.
(37) Ren, K.; Zhou, J.; Wu, H. Materials for Microfluidic Chip Fabrication. *Acc. Chem. Res.* **2013**, *46*, 2396−2406.
(38) Tang, T.; Yuan, Y.; Yalikun, Y.; Hosokawa, Y.; Li, M.; Tanaka, Y. Glass Based Micro Total Analysis Systems: Materials, Fabrication Methods, and Applications. *Sens. Actuators, B* **2021**, *339*, 129859.
(39) Karnik, R.; Gu, F.; Basto, P.; Cannizzaro, C.; Dean, L.; Kyei-Manu, W.; Langer, R.; Farokhzad, O. C. Microfluidic Platform for Controlled Synthesis of Polymeric Nanoparticles. *Nano Lett.* **2008**, *8*, 2906−2912.
(40) Legrand, P.; Lesieur, S.; Bochot, A.; Gref, R.; Raatjes, W.; Barratt, G.; Vauthier, C. Influence of Polymer Behaviour in Organic Solution on the Production of Polylactide Nanoparticles by Nanoprecipitation. *Int. J. Pharm.* **2007**, *344*, 33−43.
(41) Perrie, Y.; Webb, C.; Khadke, S.; Schmidt, S. T.; Roces, C. B.; Forbes, N.; Berrie, G. The Impact of Solvent Selection: Strategies to Guide the Manufacturing of Liposomes Using Microfluidics. *Pharmaceutics* **20192019**, *1111*, 653. Page 653
(42) Shepherd, S. J.; Issadore, D.; Mitchell, M. J. Microfluidic Formulation of Nanoparticles for Biomedical Applications. *Biomaterials* **2021**, *274*, 120826.
(43) Jordan, M. A.; Wilson, L. Microtubules as a Target for Anticancer Drugs. *Nat. Rev. Cancer* **2004**, *4*, 253−265.

https://doi.org/10.1021/acsomega.2c03137
ACS Omega 2022, 7, 33079−33086

(44) Paller, C. J.; AntonarakisCabazitaxel, E. S. A Novel Second-Line Treatment for Metastatic Castration-Resistant Prostate Cancer. *Drug Des. Dev. Ther.* **2011**, *5*, 117.
(45) Calcagno, F.; Nguyen, T.; Dobi, E.; Villanueva, C.; Curtit, E.; Kim, S.; Montcuquet, P.; Kleinclauss, F.; Pivot, X.; Thiery-Vuillemin, A. Safety and Efficacy of Cabazitaxel in the Docetaxel-Treated Patients with Hormone-Refractory Prostate Cancer. *Clin. Med. Insights Oncol.* **2013**, *7*, 1−12.
(46) Xu, A.; Yao, M.; Xu, G.; Ying, J.; Ma, W.; Li, B.; Jin, Y. A Physical Model for the Size-Dependent Cellular Uptake of Nanoparticles Modified with Cationic Surfactants. *Int. J. Nanomed.* **2012**, *7*, 3547−3554.
(47) Busatto, C.; Pesoa, J.; Helbling, I.; Luna, J.; Estenoz, D. Effect of Particle Size, Polydispersity and Polymer Degradation on Progesterone Release from PLGA Microparticles: Experimental and Mathematical Modeling. *Int. J. Pharm.* **2018**, *536*, 360−369.

https://doi.org/10.1021/acsomega.2c03137
ACS Omega 2022, 7, 33079−33086